

PREPARATION AND CHARACTERIZATION OF ALUMINUM DOPED NANOCRYSTALLINE ZINC OXIDE FOR SOLAR CELLS APPLICATIONS

J. F. MOHAMMAD*, S. M. ABED

University of Anbar, College of education for pure Sciences, Physics Department, Iraq

Undoped transparent conducting nanocrystalline Zinc oxide (ZnO) and Aluminum doped nanocrystalline Zinc oxide (Al:ZnO) thin films with three different concentrations (0.05, 0.10 and 0.15 M) of aluminum chloride (AlCl_3) have been successfully deposited on a clean commercial glass substrate using chemical bath deposition technique (CBD). The mixed aqueous solution of chemical bath consists of Zinc acetate dehydrate ($\text{Zn}(\text{CH}_3\text{COO})_2 \cdot 2\text{H}_2\text{O}$) as a source of Zn^{+2} ions and the dopant source was aluminum chloride (AlCl_3) as a source of Al^{+3} ions, while ammonium hydroxide was used to obtain an alkaline solution at a constant PH. The doping effects of aluminum chloride concentration (0.05, 0.10 and 0.15 M) on the optical and structural properties were investigated. The XRD patterns show that, all the prepared films are polycrystalline with prominent diffraction peak appear at (002) as a preferential orientation around $2\theta=34.44^\circ$. The intensity of Al doped ZnO decreased with increasing Al concentration. While atomic force microscope results appear that, the surface roughness and the grain size of the films decreased with increasing aluminum chloride concentration. From the optical measurements, the transmittance in the visible (VIS) region and optical band gap (E_g) were found to increase with increasing Al concentration. This result is attributed to the quantum size effect as expected from the nanocrystalline nature.

(Received November 15, 2018; Accepted January 23, 2019)

Keywords: Nano-thin films, CBD technique, Al- doping, Optical properties, Surface morphology

1. Introduction

In recent years, research has focused on the synthesis, characterizations and applications of nanomaterials because of their unique properties which differ from the corresponding bulk materials and play a significant role in the performance of devices [1, 2]. Among a transparent semiconductors conductive oxide (TSCO), nanostructures zinc oxide (ZnO) is a versatile material (large band gap, $E_g=3.4$ eV, large exciton binding energy (60 meV), good electrical conductivity, n-type semiconductor, high optical transparency, chemical stability, low cost and nontoxicity), these features make it excellent material match the requirement for a variety of applications such as a window layer in solar cells, transparent conductors, gas sensors, piezoelectric devices, light-emitting diodes (LED), heat mirrors etc. [3-6]. In order to improve the optical and electrical properties, especially, reduce the resistivity, ZnO nanostructures has been doped with different elements, such as aluminum (Al), gallium (Ga), indium (In), copper (Cu), Cobalt (Co) etc. The low cost and small ionic radius of Al element are considered to be an out most important dopant element [7-11]. Many techniques have been used to synthesis ZnO nanostructures such as molecular beam epitaxy (MBE) [12], sol-gel technique [13], spray pyrolysis [13], chemical vapor deposition (CVD) [14], chemical bath deposition (CBD) [15-17]. Among them, CBD technique offers unique features such as simplicity, inexpensive, low temperatures, high homogeneity and large area thin film production. In this paper, concentrations effect of Aluminum dopants on the structural and optical properties of nanocrystalline ZnO films were investigated.

* Corresponding author: jfm_67@yahoo.com

2. Experimental details

Undoped ZnO and ZnO: Al thin films (with different concentrations; 0.05, 0.10 and 0.15 M of aluminum chloride) were deposited on a clean glass substrate by using $\text{Zn}(\text{CH}_3\text{COO})_2 \cdot 2\text{H}_2\text{O}$ as a source of Zn^{+2} ions and aluminum chloride (AlCl_3) as the dopant source of aluminum ions. The molar of $(\text{Zn}(\text{CH}_3\text{COO})_2 \cdot 2\text{H}_2\text{O})$ was fixed at 0.1M during the preparation process. At 40 °C, for 30 minutes, the solutions separately dissolved in distilled water under continuous stirring using a magnetic stirrer. An appropriate amount of $(\text{NH}_4\text{OH} + \text{NH}_4\text{Cl})$ was added as a stabilizer to 20 ml of $(\text{Zn}(\text{CH}_3\text{COO})_2 \cdot 2\text{H}_2\text{O})$ to maintain PH=11 and to form a clear, homogeneous and transparent solution. The chemical bath was supplied with an air pump to obtain a certain amount of oxygen in the solution. The bath temperature was fixed at 75°C. Then, the substrate was vertically immersed in bath beaker containing the reaction mixture for deposition time 90 minutes. Finally, the prepared samples were washed with distilled water, then dried with hot air and kept in a desiccator for analysis.

3. Results and discussion

3.1. Structural properties

3.1.1. X-ray Diffraction (XRD)

Fig. 1 shows X-ray diffraction patterns of ZnO and aluminum doped ZnO thin films with (0.05, 0.10 and 0.15 M) of AlCl_3 prepared by CBD technique on glass substrates at deposition temperature 75°C for 90 minutes. As can be seen, the presence of diffraction peaks between 20° and 60° shows that the film is polycrystalline with a hexagonal wurtzite type crystal structure of ZnO. As a preferred growth orientation, the prominent peak appears at 34.44° corresponding to the (002) plane. Other orientations corresponding to (100), (101), (102) and (110) planes corresponding to the positions $2\theta=31.76^\circ$, 34.44° , 36.25° , and 47.58° respectively. The obtained XRD spectra matched well with reported standard values (JCPDS Card 00-36-1451). The crystalline structure of ZnO:Al is shown in figure 2. Clearly, the intensity of the (002) diffraction peak decreases with increasing aluminum concentration and there is a broadening in full width at half the peak maximum (FWHM) indicating that, there are nanoparticles have contributed to the X-ray diffraction. It is believed that, the decrease in grain size attributed to replacement of relatively bigger zinc ions (0.074 nm) by the relatively smaller aluminum ions (0.054 nm) during the formation of the Al-doped ZnO films which leads to decrease of the unit cell. The crystallite size (D) has been calculated using Scherer formula [18]

$$D_{hkl} = K \lambda / (\beta \cos\theta) \quad (1)$$

where;

K is a constant ($K = 0.9$), $\lambda = 1.5418 \text{ \AA}$ (λ - Wavelength of X-ray),

β - FWHM, and θ is the angle of prominent peaks.

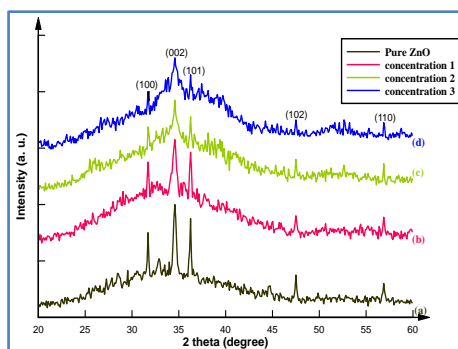


Fig. 1. XRD patterns of AZO thin films deposited with different aluminum concentrations (0.05, 0.10 and 0.15 M).

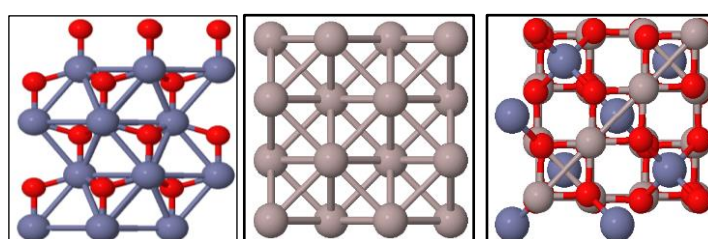


Fig. 2. Crystal structure of: (a)- Hexagonal ZnO, (b)- Aluminum and (c)- Aluminum doped zinc oxide (ZnO:Al)



3.1.2. Morphological analysis

Fig. 3 shows the scanning electron micrograph (SEM) of undoped and aluminum doped ZnO nanostructures thin films with three different concentrations (0.05, 0.10 and 0.15 M) deposited on a glass substrate. For all prepared films, the spherical grains are found to be uniform distributed completely and covered the surface of substrate without detected cracks. It is noticed that, increasing the content of aluminum in the bath solution leads to decrease the grain size. The average grain size is about 65, 53, 47 and 41 nm of undoped ZnO, AZO (0.05 M), AZO (0.10 M) and AZO (0.15 M) respectively.

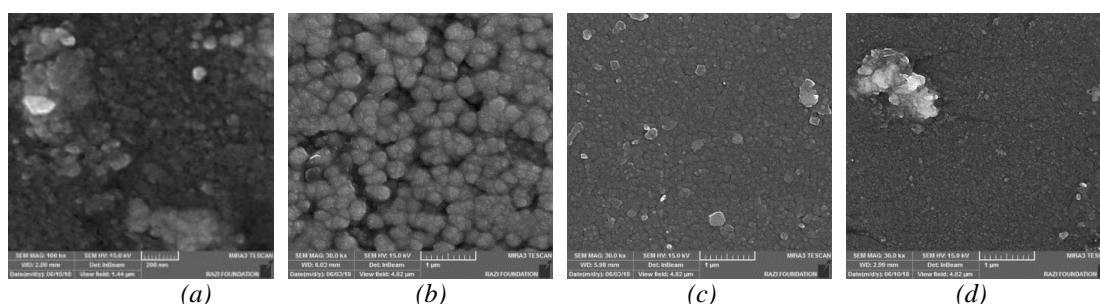


Fig. 3. SEM images of nanocrystalline thin film: (a)- Pure ZnO, (b)- ZnO:Al (0.05 M), (c)- ZnO:Al (0.10 M) (d)- ZnO:Al (0.15 M)

3.1.3. Atomic Force Microscopy (AFM) Analysis

Fig. 4 shows AFM images of undoped ZnO and Al:ZnO with three different concentrations deposited on a glass substrate. The surfaces of the prepared nanocrystalline thin films were found to be homogeneous and consists of a large number of regularly nanocrystalline

grains distributed over the entire surface. The Root-mean-square, surface roughness, ten point height and average grain size of the prepared nanocrystalline thin films were listed in Table 1. As aluminum concentration in the solution increases, the grain size and surface roughness were decreasing. This can be interpreted as follow; the aluminum affect as nucleation centers in the vacancy sites of zinc oxide which lead to decrease in thickness of these films. Smaller values of surface roughness are preferred to use these films as a transparent conducting layer in solar cell applications.

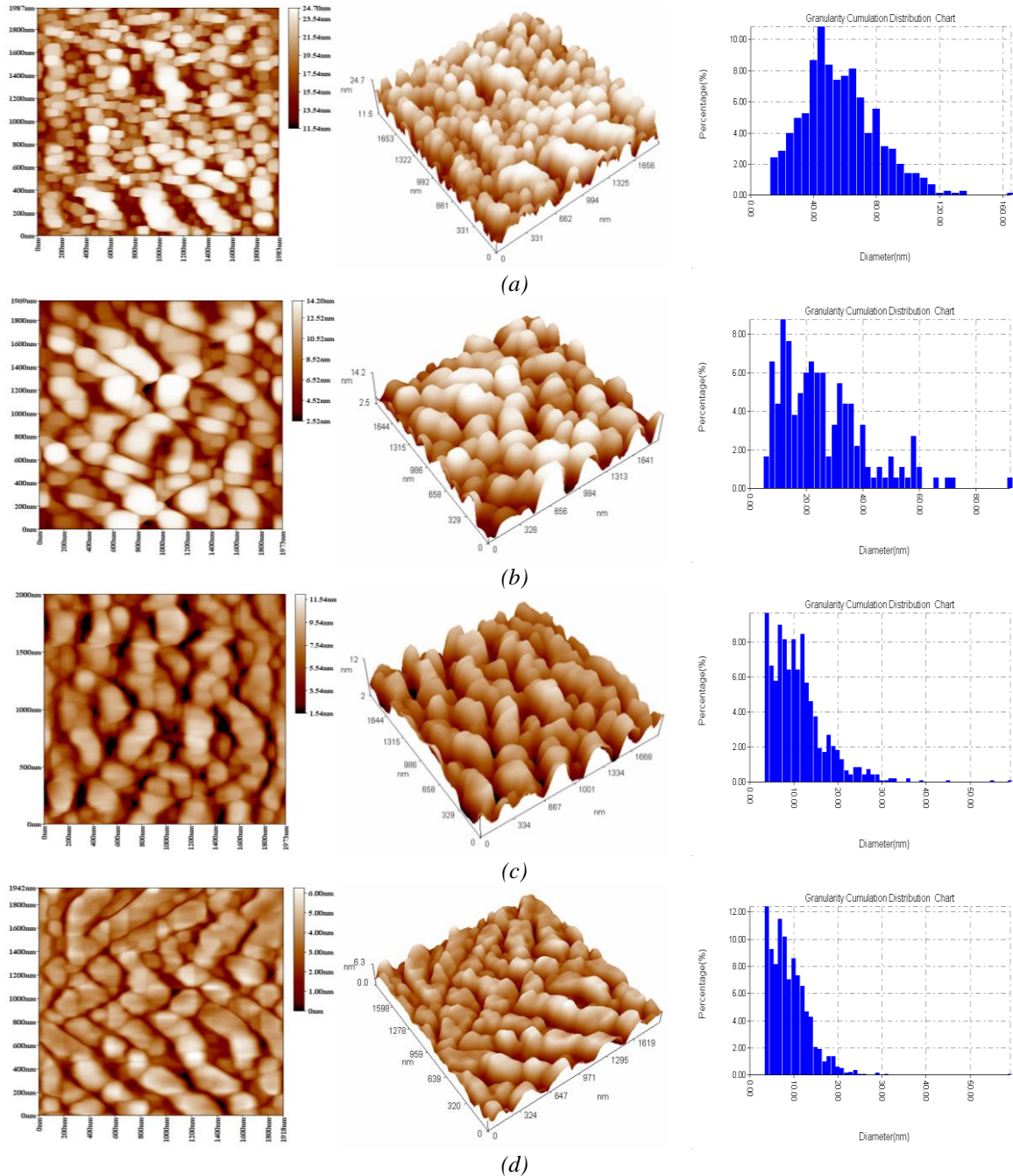


Fig. 4. AFM images of nanocrystalline thin film: (a)- Pure ZnO, (b)- ZnO:Al (0.05 M), (c)- ZnO:Al (0.10 M), (d)- ZnO:Al (0.15 M)

Table 1. The surface texture properties of the prepared samples.

Sample	Root mean square (nm)	Roughness average (nm)	Ten point height (nm)	Average grain size (nm)
Undoped ZnO	3.08	2.61	7.88	54.60
ZnO:Al (0.05 M)	2.95	2.52	7.19	25.04
ZnO:Al (0.10 M)	2.32	1.94	6.31	10.69
ZnO:Al (0.15 M)	1.19	0.958	6.05	8.72

3.2. Optical properties

The transmission spectra measurement has been investigated by using UV-VIS spectrophotometer in the range of (300-1100 nm.) at room temperature. Fig. 5 shows the optical transmittance as a function of wavelength of the undoped noncrystalline ZnO and Al doped ZnO thin films with (0.05, 0.10 and 0.15 M) of aluminum chloride deposited on glass substrate using the CBD technique at a bath temperature 75 °C. The average transmittance, in the visible region, is greater than 80 %. It is clear that, the transmittance increase when ZnO is doping with Al, this is may be denoted the decrease in film thickness. This feature makes these films applicable for optoelectronic devices such as a conducting layer for solar cells.

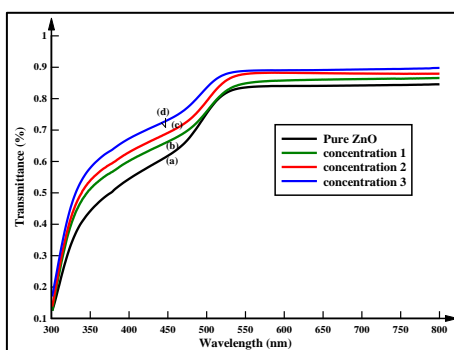


Fig. 5. Transmittance versus wavelength of nanocrystalline thin film: (a)- Undoped ZnO, (b)- ZnO:Al (0.05 M), (c)- ZnO:Al (0.10 M), (d)- ZnO:Al (0.15 M).

The absorption coefficient (α) versus wavelength of undoped noncrystalline ZnO and Al:ZnO thin films with three different aluminum chloride concentrations (0.05, 0.10 and 0.15 M) were determined from absorbance measurements by using equation (1).

$$\alpha = \frac{2.3026 A}{t} \quad (1)$$

Where: A - is the absorbance and, t – Thickness of the film.

The absorption coefficient of undoped noncrystalline ZnO thin film decreases with the increasing of AlCl_3 concentration in the solution as shown in Fig. 6. This means that, the absorbance of doped films are decreasing with concentration increasing of aluminum chloride as is evident from equation (1). In solar cell applications, one of the important conditions is that the absorption factor is as low as possible. According to the results, these films are suitable for use in solar cells.

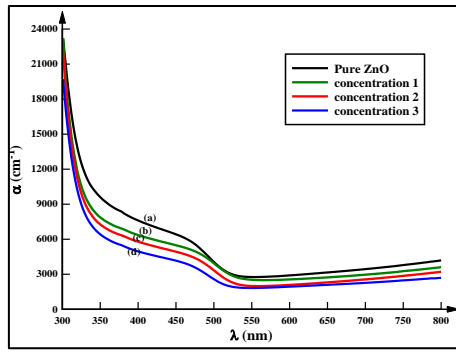


Fig. 6. Absorption coefficient versus wavelength of nanocrystalline thin film: (a)- Undoped ZnO, (b)- ZnO:Al (0.05 M), (c)- ZnO:Al (0.10 M), (d)- ZnO:Al (0.15 M)

The optical energy gap (E_g) of nanocrystalline pure ZnO and Al doped ZnO thin films, which have been determined using the following equation:

$$\alpha h\nu = A (h\nu - E_g)^n \quad (3)$$

where A is a constant, the best linear fit is obtained for $n = 1/2$. The relation is plotted between $(\alpha h\nu)^2$ and $(h\nu)$, as shown in Fig. 7, which illustrates allowed direct electronic transition. Energy gap was determined by the extrapolation of the portion at $(\alpha=0)$. It is clear that, the optical energy gap (E_g) increases with increasing aluminum chloride concentration in the solution and E_g shifts towards the higher photon energy region. This is attributed to decreasing in grain size of the doped films, which causes substitution of Al ions in the undoped ZnO lattice. The optical energy gap values of undoped nanostructure ZnO, AZO (0.05 M), AZO (0.10 M) and AZO (0.15 M) thin films were 3.65, 3.72, 3.75 and 3.8 eV respectively. The increase in energy gap is attributed to quantum size effect, which related to nano-size of the grains.

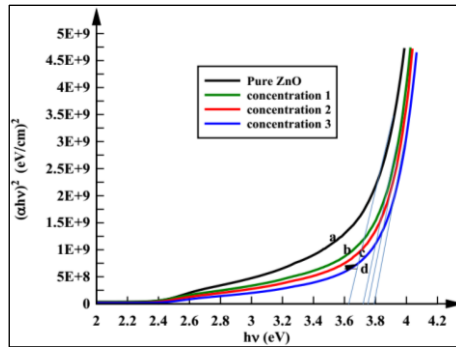


Fig. 7. Optical energy gap versus wavelength of nanocrystalline thin film: (a)- Undoped ZnO, (b)- ZnO:Al (0.05 M), (c)- ZnO:Al (0.10 M), (d)- ZnO:Al (0.15 M).

4. Conclusions

Undoped nanocrystalline ZnO and aluminum doped ZnO thin films are successfully deposited on glass substrate using CBD technique. The structural and morphological results showed that the prepared films have a nanocrystalline structure, polycrystalline nature and the grains are well covered the surface of the substrate of each sample. Also the films have a low roughness. While the optical results showed the transmittance greater than 80 % and the values of energy gap were; 3.65, 3.72, 3.75 and 3.8 eV for nanostructure ZnO, AZO (0.05 M), AZO (0.10 M) and AZO (0.15 M) thin films respectively. These results show that doping have altered and

improved the properties of the films in order to be suitable in solar cells and other optoelectronic applications.

References

- [1] M. S. Ghamsari, S. Radiman, M. A. A. Hamid, S. Mahshid, Sh. Rahmani, *Materials Letters* **92**, 287 (2013).
- [2] S. Suwanboon, T. Ratana, T Ratana, *Walailak Journal of Science and Technology* **4**, 111 (2007).
- [3] F. Benharrats, K. Zitouni, A. Kadri, B. Gil, *Superlattices and Microstructures* **47**, 592 (2010).
- [4] A. Mhamdi, A. Boukhachem, M. Madani, H. Lachheb, K. Boubaker, A. Amlouk, M. Amlouk, *Optik* **124**, 3764 (2013)
- [5] K. L. Chopra, P. D. Paulson, V. Dutta, *Prog. Photovoltaics: Res. Appl.* **12**, 69 (2004).
- [6] K. Nomura, H. Ohta, A. Takagi, T. Kamiya, M. Hirano, H. Hosono, *Nature* **432**, 488 (2004).
- [7] S. Benramache, B. Benhaoua, F. Chabane, *Journal of Semiconductors* **33**, 093001 (2012).
- [8] X. B. Wang, C. Song, K. W. Geng, F. Zeng and F. Pan, *J. Phys. D Appl. Phys.* **39**, 4992 (2006).
- [9] F. Wang, M. Z. Wu, Y.Y. Wang, Y.M. Yu, X.M. Wu, L.J. Zhuge, *Vacuum* **89**, 127 (2013).
- [10] M. Q. Bao, Z. Z. Ye, H. P He, J. R. Wang, L. P. Zhu, B. H. Zhao, *Materials Characterisations* **59**, 124 (2008).
- [11] O. Lupan, T. Pauport'e, T. Le Bahers, I. Ciofini and B. Viana, *J. Phys. Chem. C* **115**, 14548 (2011).
- [12] D. Vernardou, G. Kenanakis, S. Couris, A. C. Manikas, G. A. Voyiatzis, M. E. Pemble, E. Koudoumas, N. Katsarakis, *Journal of Crystal Growth* **308**, 105 (2007).
- [13] J. Ramesh, G. Pasupathi, R. Mariappan, V. Senthil Kumar, V. Ponnuswamy, *Optik* **124**, 2023 (2013).
- [14] S. Benramache, B. Benhaoua, N. Khechai, F. Chabane, *Mater. Techniq.* **100**, 573 (2012).
- [15] S. H. Chiu, J. C. A. Huang, *Journal of Non-Crystalline Solids* **358**, 2453 (2012).
- [16] R. Zhang and L. L. Kerr, *J. Solid State Chem.* **180**, 988 (2007).
- [17] D. Chu, T. Hamada, K. Kato, Y. Masuda, *Physical Status Solidi A* **206**, 718 (2009).
- [18] H. P. Klug, L. E. Alexander, *X-ray diffraction procedures for polycrystalline and amorphous materials*, Wiley, New York, 1974.